Springer

KSME

Journal of Mechanical Science and Technology 32 (6) (2018) 2497~2507
www.springerlink.com/content/1738-494x(Print)/1976-3824(Online)
DOI 10.1007/s12206-018-0507-z

Prediction of remaining useful life under different conditions using accelerated life testing data †

Dawn An[1], Joo-Ho Choi[2,*] and Nam Ho Kim[3]

[1]*Korea Institute of Industrial Technology, Yeongcheon-si, Gyeongbuk-do 38822, Korea*
[2]*Korea Aerospace University, Goyang-si, Gyeonggi-do 412-791, Korea*
[3]*University of Florida, Gainesville, FL, 32611, USA*

(Manuscript Received February 14, 2018; Revised March 26, 2018; Accepted April 16, 2018)

Abstract

Prognostics methods model the degradation of system performance and predict remaining useful life using degradation data measured during service. However, obtaining degradation data from in-service systems in practice is either difficult or expensive. Therefore, accelerated life testing (ALT) is instead frequently performed for validating designs using considerably heavy loads. This work discusses the methods and effectiveness of utilizing ALT degradation data for the prognostics of a system. Depending on the degradation model and loading conditions, four different ways of utilizing ALT data for prognostics are discussed. A similar transformation method used in ALT is adopted to convert accelerated loading conditions to field loading conditions. To demonstrate the proposed approach, synthetic data are generated for crack growth under accelerated loading conditions; these data are used for training a neural network model or identifying model parameters in a particle filter. The applied example shows that the use of ALT data increases the accuracy of prognostics in the early stages in all four cases and compensates for the problem posed by data insufficiency through the proposed method.

Keywords: Accelerated life testing; Prognostics; Neural network; Particle filter

1. Introduction

The performance of a system degrades over time. Prognostics uses degradation/damage data obtained in service to model the degradation behavior. The model aims to estimate the time for maintenance. The time to the next maintenance is called the remaining useful life (RUL). The system is considered to perform its intended function until RUL. A general process of prognostics is shown in Fig. 1. Once degradation data are collected from the in-service system, physics-based prognostics first determines the parameters of the damage model under given loading conditions using degradation data (black dots) up to the current time k and then predicts the RUL. Data-driven prognostics uses degradation data under similar/different usage conditions (gray dots) to train mathematical models. Due to various sources of uncertainty, such as measurement variability, model form uncertainty, and usage conditions, the predicted RUL often shows a statistical distribution.

Compared to scheduled maintenance, condition-based maintenance (CBM) using prognostics [1] is safe and cost-effective. However, several challenges remain in making CBM practical in industry. An et al. [2] summarized several challenges in prognostics. Among them, the issue of the limited number of data during field operation is the focus here. In practice, field degradation data are rare, and their acquisition is either difficult or expensive. This study aims to utilize damage data measured during accelerated life testing (ALT) for system health management and prognostics. Most companies have many ALT data because these are frequently used to validate designs. However, ALT data cannot be used for prognostics directly because loading conditions considerably differ from field loading conditions.

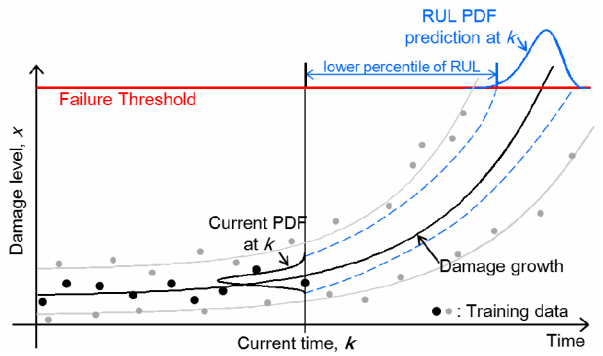

Fig. 1. Illustration of prognostics process with training data.

*Corresponding author. Tel.: +1 352 575 0665, Fax.: +1 352 392 7303
E-mail address: jhchoi@kau.ac.kr
† This paper was presented at PHMAP 2017, Ramada Plaza Jeju Hotel, Jeju, Korea, July 12 - 15, 2017. Recommended by Guest Editor Suk Joo Bae.

Many previous studies have covered life estimation using ALT data [3, 4], which focus on validating designs and estimating the average life of systems. Degradation data during ALT are also used for prognostics by ignoring the difference between accelerated loading conditions and field loading conditions. Estimating the useful life under field conditions is challenging because ALT conditions differ from field conditions [5]. When physics-based models that describe degradation behavior are available, ALT data can be used with ALT loading conditions because the major task is to identify model parameters [6]. ALT data have also been used to build a mathematical model for data-driven methods [7]. However, predicting the RUL without converting ALT loading conditions to real field conditions is generally difficult.

In this paper, four different ways of utilizing ALT degradation data are presented to predict degradation in terms of the RUL of a system under field loading conditions. The individual methods are categorized depending on the amount of information available, such as the availability of degradation models and/or field operation loading conditions. Several cases are available in the literature; however, the last case in this work is unique because no physics-based models and field loading conditions are given. In such a case, a mapping method that can compensate for insufficient field data using a data-driven approach must be introduced. Although other scenarios are not new, they are also discussed here.

During ALT, damage growth is closely monitored using sensors or scheduled inspections until it reaches a threshold, which is the level of damage at which the system cannot function unless the damage is fixed. The current system measures damage up to the current time using onboard sensors. However, with the current system alone, the number of degradation data is not enough to accurately predict the RUL. The RUL must be predicted such that the system can undergo maintenance before it becomes inoperable. Prognostics involves numerous uncertainties. Hence, RUL prediction must be given as a probability distribution, and maintenance can be performed on the basis of the level of risk.

This paper is organized as follows. Two prognostics approaches are reviewed in Sec. 2. Sec. 3 introduces the crack growth example used to explain the proposed methods. Sec. 4 explains how ALT data are used for four different cases. The conclusions in Sec. 5 summarize the four proposed cases.

2. Review of prognostics approaches

In general, three prognostics methods are available: Physics-based [8], data-driven [9], and hybrid [10] approaches. The difference lies in the use of information. Defining hybrid approaches is difficult. Hence, only data-driven and physics-based approaches are discussed in this section. The two approaches differ in (1) whether a physical model is available to describe the degradation behavior, (2) whether the usage or loading conditions in the field are available, and (3) whether training data are used to predict the damage growth. Detailed explanations for the two approaches are provided in the following subsections.

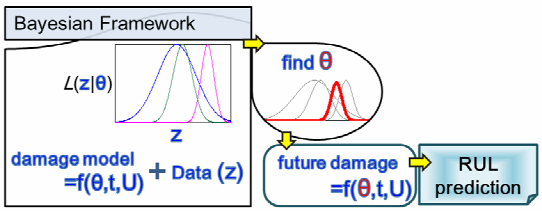

Fig. 2. Illustration of physics-based prognostics.

2.1 Review of physics-based approaches

Physics- or model-based approaches use degradation models that describe the behavior of degradation, estimate unknown model parameters with degradation data, and predict the future behavior of damage. The process of physics-based prognostics using the Bayesian framework is shown in Fig. 2. The damage degradation behavior is described as a function of usage or loading conditions U, operation cycles or time t, and the model parameters $\boldsymbol{\theta}$. The usage/loading conditions and operation time are normally given. Thus, identifying the unknown model parameters is the most important step in predicting the RUL. Therefore, physics-based prognostics algorithms are categorized on the basis of parameter estimation methods. Bayesian inference-based methods [11] are the most popular, including the Kalman filter [12], extended Kalman filter [13], particle filter [14], and Bayesian method [15].

In physics-based prognostics methods, the Bayesian method is often used to infer unknown model parameters using measured data. The uncertainty is represented using a probability density function (PDF). Bayesian inference is a special form of Bayes' theorem, which can be expressed as follows [11]:

$$p(\boldsymbol{\theta}|\mathrm{z}) \propto L(\mathrm{z}|\boldsymbol{\theta})\, p(\boldsymbol{\theta}), \tag{1}$$

where $p(\boldsymbol{\theta}|\mathrm{z})$ is the posterior PDF of model parameters $\boldsymbol{\theta}$ conditional on measured data z, $L(\mathrm{z}|\boldsymbol{\theta})$ is the likelihood function, and $p(\boldsymbol{\theta})$ is the prior PDF. The likelihood function represents the probability of obtaining data z with the parameters assumed to be $\boldsymbol{\theta}$. Any prior information, such as experts' opinion or the range of generic material properties from a material handbook, can be represented in the prior PDF. When no prior information is available, $p(\boldsymbol{\theta})$ can be ignored, which is also referred to non-informative prior. The uncertainty in the posterior PDF can be decreased when additional data are used. Thus, the RUL can be predicted precisely.

Any physics-based algorithm can be used, but the particle filter algorithm is considered here because of its popularity. The particle filter algorithm sequentially estimates and updates model parameters with data. The posterior PDF is expressed in the form of many particles and their weights. Detailed explanations of the particle filter algorithm can be found

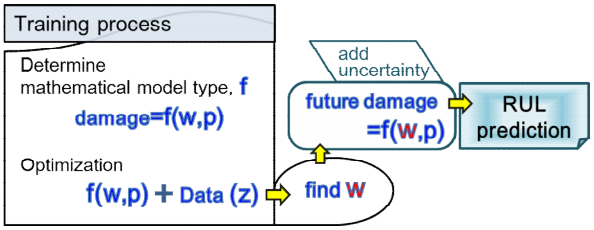

Fig. 3. Illustration of data-driven prognostics.

in the Refs. [14, 16, 17].

Loading conditions for ALT are known. Hence, physics-based approaches can be applied without any modification to estimate model parameters. However, the assumption is that the model parameters of the system used in ALT are the same as those of the current machine. The accuracy of predicting the RUL can be affected by the difference in system model parameters caused by manufacturing variability.

2.2 Review of data-driven approaches

Data-driven approaches are advantageous when no reliable degradation model is available or the model is too complex. These approaches use collected data from similar systems (training data) to train a mathematical model, from which the RUL can be predicted. Data-driven algorithms can be divided into two categories: (1) Artificial intelligence approaches that include fuzzy logic [18] and neural networks [19, 20]; and (2) statistical approaches that include gamma processes [21], hidden Markov models [22], and regression-based models. Regression models include the Gaussian process [23, 24], relevance vector machine [25], and least squares regression [26].

As shown in Fig. 3, data-driven approaches are a regression comprising a mathematical model (f), input variables (p), and parameters (w). The model f relates the input variables to the output damage state mathematically but does not represent any physics. This relationship can be established in numerous ways. In this work, an incremental relationship between consecutive damage states is generated, where the damage states at previous times are used as input variables. In addition to damage states at previous times, the loading condition can be included if available, thereby potentially increasing prediction accuracy. Once the form of the mathematical model is fixed, its parameters can be estimated by minimizing the discrepancy between the damage states predicted by the model and the measured ones. The data used for identifying the parameters are called training data. Training data are obtained from similar systems under the same or different loading conditions. Fig. 1 shows the training data in gray dot markers. The training data can also be obtained from the current system at previous times under a given usage condition, as shown by the black dot markers in Fig. 1. The estimated model parameters can be used to predict the future damage state and the RUL. The mean-squared-error between training outputs and training data is used as a measure of uncertainty in prediction.

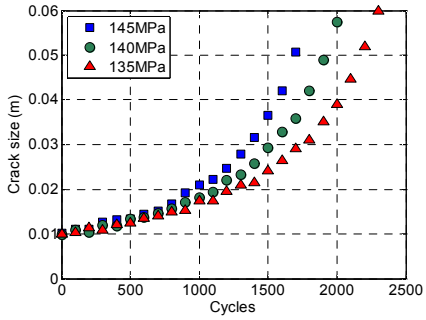

(a) Accelerated life tests

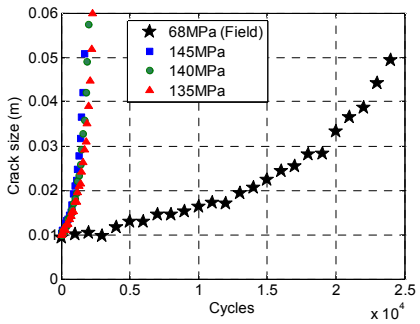

(b) Field operating conditions

Fig. 4. Crack growth data under various loading conditions (simulated measurement by addition of random noise).

Among the many data-driven algorithms, neural networks are the most commonly used. A typical neural network model comprises several input and hidden nodes and one output node. A detailed explanation of neural network models can be found in the Refs. [2, 27]. For demonstration purposes, the neural network model in Sec. 4 is constructed with three input nodes and two hidden nodes with one hidden layer. The damage data at the three previous times are used for the input layer. For the transfer functions, the pure linear and tangent sigmoid functions are used. When the measured previous damage data are used as input, the prediction will be one step ahead (short-term prediction). The predicted damage states can be used as input to predict the damage state in a future time (long-term prediction).

The number and quality of training data are the major factors behind the performance of data-driven approaches. Hypothetically, the best scenario is when accurate degradation data of the same system under the same loading conditions are available. In practice, however, such a scenario is unlikely. Therefore, this study aims to show that ALT data from different loading conditions can be used as training data. A technical challenge is how ALT data, which are obtained under loading conditions that differ from field loading conditions, can be used for training the current system.

3. Demonstration example: Fatigue crack growth

A small initial crack on the fuselage panel of aircraft can

grow over time under repeated pressurization loadings. This situation is used as a demonstration example in this work. The crack is the damage, and the size of the crack is the damage state. When the crack size reaches a threshold, the panel is considered failed. Therefore, maintenance needs to be conducted before the crack size reaches the threshold.

For physics-based prognostics, the growth of a crack can be modeled using the following Paris model [28]:

$$\frac{da}{dN} = C(\Delta K)^m, \ \Delta K = \Delta\sigma\sqrt{\pi a}, \tag{2}$$

where da/dN is the rate of crack growth with the half crack size a and the number of loading cycles N; m and C are Paris model parameters; ΔK is the range of mode 1 stress intensity factor; and $\Delta\sigma$ is the stress range due to the pressure differential. The rate of crack growth depends on the model parameters and the loading conditions $\Delta\sigma$.

Obtaining real data is difficult. Thus, measurement data are simulated using Eq. (2) with the following assumed true parameters: $m_{\text{true}} = 3.5$, $C_{\text{true}} = 6.4\times10^{-11}$, and initial half crack size $a_0 = 10$ mm. These true parameters are used only for generating simulated data and verifying the accuracy of estimated parameters.

For the demonstration example, ALT is assumed to be conducted at three stress ranges, $\Delta\sigma$ = 135, 140 and 145 MPa, while the real operating condition is with $\Delta\sigma$ = 68 MPa. A uniformly distributed random noise between $\pm u$ mm is added to the crack growth data in Eq. (2) to consider the real measurement environment. The laboratory environment for ALT is controlled better than the field operating environment. Hence, u = 0.7 mm is used for ALT data, and u = 1.5 mm is adopted for the field loading condition. Fig. 4 shows the damage degradation data generated for the demonstration problem. The three markers in Fig. 4(a) represent the three sets of ALT data at high-stress ranges, which are used to increase the accuracy of prognostics along with the measured damage data of the current system, which are depicted by star markers in Fig. 4(b). This study is unique in that the ALT data in Fig. 4(a) are used to predict the damage state under field loading conditions with considerably low stress levels in Fig. 4(b).

4. Four scenarios of using accelerated life test data for prognostics

Four ways of utilizing ALT data are presented in this section. As listed in Table 1, these techniques differ in terms of the availability of information about physical models and field loading conditions. Cases 1 and 4 assume the most and least information, respectively. In case 4, a new method is proposed to utilize ALT data effectively.

4.1 Case 1: Physical model + field loading information

When the number of data is the same, physics-based prognostics algorithms are preferred to data-driven ones. Therefore, the use of physics-based algorithm is always recommended when a physical model that describes the behavior of damage is available. In general, physics-based prognostics algorithms can predict damage behavior without utilizing ALT data. These algorithms can improve prognostics accuracy and reduce uncertainty in early-stage prognostics because ALT data can be used to generate good prior information for the model parameters.

Table 1. Four scenarios considered in numerical study (PF: Particle filter, NN: Neural network).

	Case 1	Case 2	Case 3	Case 4
Physical model	O	O	X	X
Field loading	O	X	O	X
Available method	Physics-based (PF)		Data-driven (NN)	

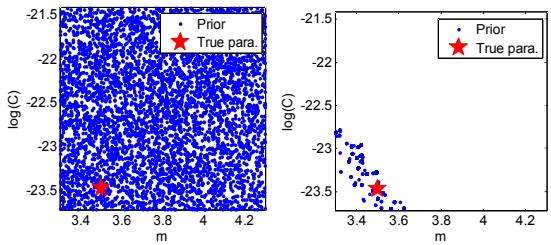

(a) From literature (b) From ALT

Fig. 5. Prior distributions of two Paris model parameters.

To show how to utilize ALT data in physics-based prognostics, consider that the Paris model parameters m and C in Eq. (2) need to be estimated for the fuselage panel of an airplane. As prior information, the values from a generic Al 7075-T651 material are used. Newman et al. [29] provided the lower and upper bounds of these parameters that are due to material variability. In the current work, the exponent m and the logarithm of C are assumed to be uniformly distributed; that is, $m \sim U(3.3, 4.3)$ and $\log(C) \sim U\left(\log\left(5\times10^{-11}\right), \log\left(5\times10^{-10}\right)\right)$. Fig. 5(a) shows 5000 samples of m and C, where the true values of the two parameters are denoted by star markers. The true value must be determined using crack growth measurement data. The uncertainty in the initial uniform distribution in Fig. 5(a) is so large that it fails to provide useful information for predicting the crack growth.

Although any physics-based prognostics algorithm can be used, the particle filter is used in this paper to demonstrate how to utilize ALT data. In the current airplane, the ALT data may not be accurate because they are not from the same panel of the same airplane. Therefore, ALT data are used only for reducing the uncertainty in the prior distribution of m and C. After updating the initial distribution with the three sets of ALT data in Fig. 4(a), a narrow prior distribution shown in Fig. 5(b) is obtained. The updated prior in Fig. 5(b) is considerably narrower than the initial uniform distribution in Fig. 5(a). The updated distribution does not converge toward the true values because the two model parameters are strongly correlated.

Table 2. Prognostics metrics for case 1.

	PH ($\alpha = 10\,\%$)	α-λ accuracy ($\alpha = 10\,\%$, $\lambda = 0.5$)	RA ($\lambda = 0.5$)	CRA
Prior from literature	11000	False (0.2504)	0.9161	0.8479
Prior from ALT data	**21000**	**True (0.6046)**	**0.9240**	**0.9285**

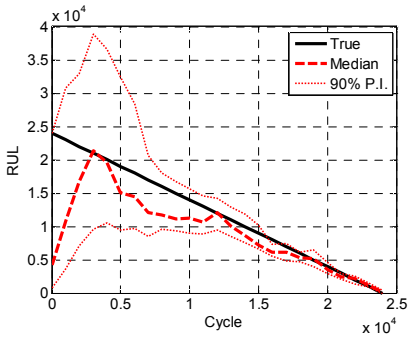

(a) Based on prior from literature

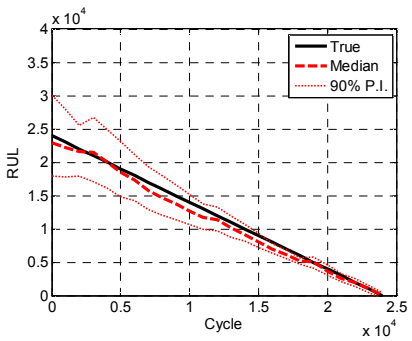

(b) Based on prior from ALT

Fig. 6. RUL prediction of case 1.

Instead, the updating process in the particle filter becomes a narrow band between the two parameters. As claimed by An et al. [30], the crack propagation will be the same if any combination within the band is used. The advantage of using ALT data for physics-based prognostics is that the prognostics can start with a narrow prior distribution, as shown in Fig. 5(b).

To evaluate the effect of ALT data, the two prior distributions in Figs. 5(a) and (b) are used, and the particle filter algorithm is adopted to estimate the posterior distributions with the field-measured data. Then, these distributions are used to predict the RUL. Fig. 6(a) shows the median and 90 % prediction intervals of RUL when the uniformly distributed prior in Fig. 5(a) is used. Fig. 6(b) is the case where the prior information from the ALT data in Fig. 5(b) is applied. Accurate and precise predictions are obtained at an early stage because the prior information is precise. Table 2 compares the two RUL results in terms of the prognostics metrics [31]. The larger the prognostics metrics, the better the prediction. In all metrics, using the prior from ALT data is better than using uniformly distributed prior from the literature.

4.2 Case 2: Physical model + no field loading information

In addition to the physics-based model, the available loading condition is also a unique feature of physics-based prognostics approaches. Loading conditions can significantly affect the evolution of degradation. The loading condition in ALT is relatively well identified as a specific load (or the history of loads) is applied to the system. In the field, however, measuring the real operating loads is difficult, and the loads may not be constant. Therefore, case 2 corresponds to the case when the degradation model is available (albeit its model parameters need to be estimated) but the field loadings are unknown. For simplicity of presentation, this work considers the case where the field loading is constant but its magnitude is unknown.

The field operation loading, which is unknown, must be estimated using the same process as the model parameters. The prior distribution of the loading is assumed uniformly distributed between 50 and 90 MPa, while the true loading is 68 MPa. With a given degradation model, two ways of predicting the RUL are considered: (A) Updating parameters and loadings simultaneously and (B) updating loadings with a fixed distribution of parameters.

For case 2-A, the prior distribution of the model parameters can be either that in Fig. 5(a) or in Fig. 5(b). Then, the data from field operation are used to update the model parameters and uncertain loading conditions. Therefore, the particle filter algorithm updates the joint PDF of all three variables with field data. Fig. 7 and Table 3 show the comparison of the RUL prediction using the two priors given in Figs. 5(a) and (b). Although the difference is not clear in the graph, the prognostics metrics in Table 3 show that the case with the prior from ALT data yields slightly better results than that using the prior from the literature. The improvement is small for a narrow prior in Fig. 5(b) because of the correlation between model parameters and loading. Even if the case with a uniform prior in Fig. 5(a) may converge slowly in finding accurate values of the parameters and loading, the predicted RUL can be accurate when the correlation is well identified. In addition, the number of field data is large enough to identify the correlation structure between model parameters and loading condition. However, if many model parameters are present and correlation relationships among parameters are complex, then narrow priors may outperform uniform priors.

In case 2-A, the model parameters and uncertain loading conditions are updated using the field-measured data. In case 2-B, only uncertain loading conditions are updated; the model parameters remain the same with the prior distribution in either Fig. 5(a) or 5(b). Fig. 8 and Table 4 show that utilizing the prior distribution from ALT significantly improves the performance of prognostics. The best prediction among all cases is also shown (Tables 3 and 4). In addition, the estimated loading converges to the true value because the correct ALT loading information is applied.

Table 3. Prognostics metrics for case 2-A.

	PH ($\alpha = 10\,\%$)	α-λ accuracy ($\alpha = 10\,\%$, $\lambda = 0.5$)	RA ($\lambda = 0.5$)	CRA
Prior from literature	11000	False (0.3246)	0.8739	0.8116
Prior from ALT data	**13000**	False **(0.4728)**	**0.9704**	**0.8643**

Table 4. Prognostics metrics for case 2-B.

	PH ($\alpha = 10\,\%$)	α-λ accuracy ($\alpha = 10\,\%$, $\lambda = 0.5$)	RA ($\lambda = 0.5$)	CRA
Prior from literature	2000	False (0.0578)	0.4627	0.4450
Prior from ALT data	**11000**	**True (0.5182)**	**0.9727**	**0.8751**

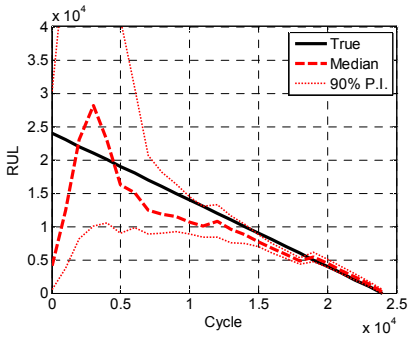

(a) Based on prior from literature

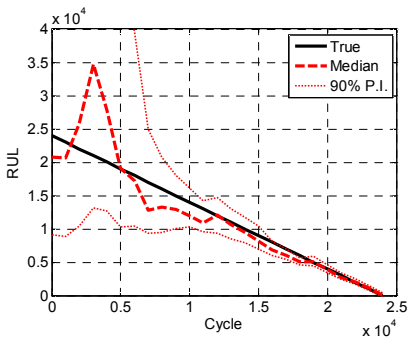

(b) Based on prior from ALT

Fig. 7. RUL prediction of case 2-A.

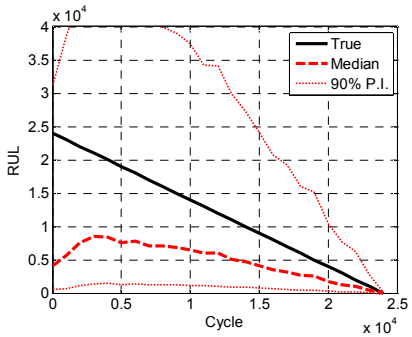

(a) Based on prior from literature

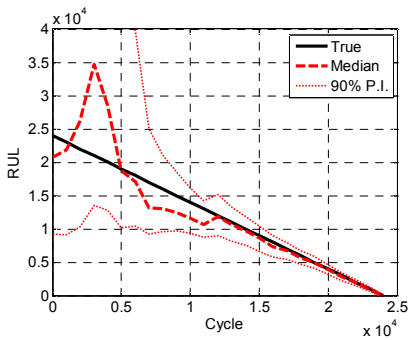

(b) Based on prior from ALT

Fig. 8. RUL prediction of case 2-B.

4.3 Case 3: No physical model + field loading information

Case 3 corresponds to the case where the physical model is not available but the field loading conditions are known. Since no physics-based model is available, a data-driven approach must be chosen. Among different data-driven approaches, the neural network is utilized in this paper. In addition to damage growth information, loading conditions are added to the input variables. This addition is particularly important because the ALT data are under different load levels, and the neural network must consider the varying damage growth rates under different load levels.

Fig. 9 shows the prognostics results obtained without the use of ALT data. In this case, only damage data from field loading conditions are used for training the network. The median of prediction results (red dashed lines) approach the true damage growth (black solid lines), and the prediction intervals (red dotted lines) become narrow as the number of cycles increases from 10000 to 18000. However, the prediction results cannot keep up with the rapidly growing true damage even at 18000 cycles because the damage grows slowly in the training data relative to the damage at the prediction cycles.

When the training data include ALT data, the prediction results are better than those obtained without use of ALT data, as shown in Fig. 10. The prediction uncertainties are remarkably high because of the large difference in degradation rates between ALT and field data. However, the prediction results obtained using ALT data in Fig. 10 are more reliable than those obtained without ALT data in Fig. 9, considering that the decision for maintenance is usually made on the basis of the lower bound of prediction results. This finding is supported by the results of RUL and prognostics metrics, as shown in Fig. 11 and Table 5. These results show that using ALT data for training is beneficial even when loading conditions differ.

4.4 Case 4: No physical model + no field loading information

Case 4 is the most difficult but also practical case because it requires the least amount of information. Data-driven prog-

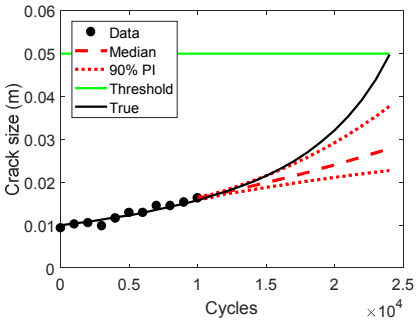

(a) At 10000 cycles

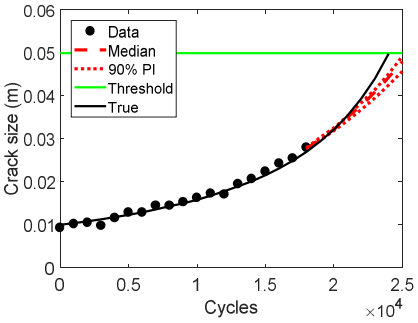

(b) At 18000 cycles

Fig. 9. Damage predictions without using ALT data.

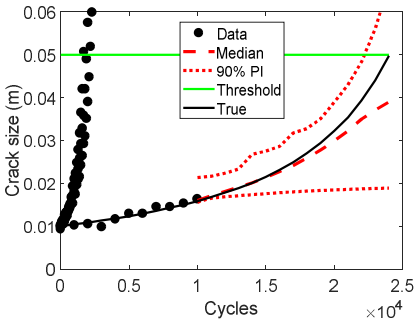

(a) At 10000 cycles

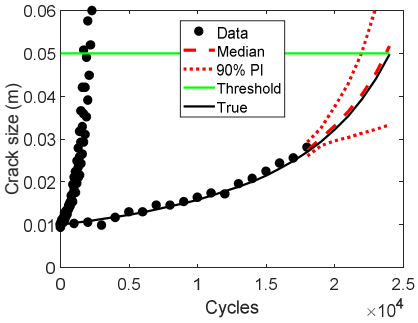

(b) At 18000 cycles

Fig. 10. Damage prediction using ALT data with loading information (case 3).

nostics (neural network algorithm) is adopted because no degradation model is available. In general, data-driven approaches require a large volume of training data under the same or similar usage/loading conditions with the field condition because they do not use physical degradation models. Measuring degradation data is expensive. Therefore, degradation data measured during ALT are transformed into those at the field loading condition instead so that they can be considered as training data for the prognostics of the current in-service system.

Table 5. Prognostics metrics for case 3.

	PH ($\alpha = 10\,\%$)	α-λ accuracy ($\alpha = 10\,\%$, $\lambda = 0.5$)	RA ($\lambda = 0.5$)	CRA
Without ALT data	4000	False (0.0000)	0.5239	0.5210
Case 3	**9000**	False (**0.0333**)	**0.5445**	**0.7810**

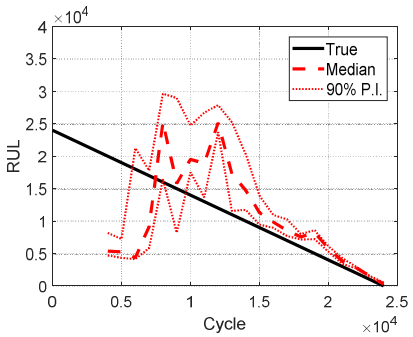

(a) Without using ALT data

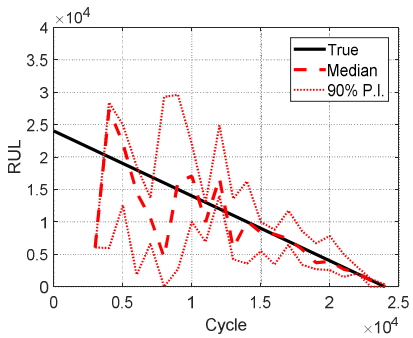

(b) Using ALT data with loading information

Fig. 11. RUL prediction (case 3).

The inverse power model in ALT [3] is adopted to transform the ALT data to field-measured data that can be used for training. This model is commonly used in such applications as metal fatigue, bearings, and electric insulators. The model is mostly used to estimate life under different loading conditions. In this study, the model is used to transform ALT data to field loading condition data. The inverse power model [3] is linear between the applied load and the logarithm of life.

$$Life = \frac{\alpha}{Load^{\beta}}, \quad \log(Life) = \log(\alpha) - \beta \log(Load), \tag{3}$$

where $Life$ is the lifespan of a system and α, β are unknown coefficients. The coefficients are estimated using lifespan data under different usage/loading conditions. Once these

coefficients are estimated, the lifespan under field loading conditions can be obtained from Eq. (3). The above relationship is widely used for design validation using ALT. This relationship has not been used for prognostics, particularly for generating training data for data-driven prognostics.

The coefficients α, β in Eq. (3) need to be estimated before the inverse power model is applied. The lifespan is the time consumed as the damage reaches the threshold. In this study, 50 mm is used as the threshold and shown as a horizontal dashed line in Fig. 12(a). On the basis of this threshold, the lifespans of three load levels, 145, 140 and 135 MPa, are respectively determined as 1734, 1947 and 2241 cycles, respectively; these lifespans are indicated by three markers in Fig. 12(b). The parameters of the inverse power model are the slope β and y-intercept $\log(\alpha)$ of the line connecting these three markers. To build the model, at least two sets of data for different loading levels should be available. When more than two sets are available, the line can be found using regression.

Once $\log(\alpha)$ and β are found, the lifespan at the field loading can be calculated using the inverse power model in Eq. (3). The star markers in Fig. 12(c) show the transformed lifespan at different load levels from 50 MPa to 90 MPa at 5 MPa increments. The same process can be repeated by gradually changing the threshold to obtain the solid curves in Fig. 12(c), which are the damage growth curves for a given load. However, the range of load (50 MPa to 90 MPa) is too wide because, as shown in Fig. 12(c), the rates of damage growth are significantly different over the range. The range of loading can be reduced by comparing the mapped damage curve with the field-measured damage data. Although all data between 50 and 90 MPa can be used for training, the use of data that are close to the field loading conditions is recommended. Without knowing the field loading conditions, data can still be selected from 65, 70 and 75 MPa because their damage growths are close to the field-measure damage growth rate. Therefore, these three sets of transformed data are used for training.

The above three steps of transformation in Figs. 12(a)-(c) involve the following three sources of uncertainty.

(1) Uncertainty in the regression process of ALT data: The first step is conducting regression to calculate the lifespan using ALT data, which are given at every 100th cycle in terms of damage size (markers in Fig. 12(a)). For a given loading, the regression process is repeated 30 times, where the initial weights and training data are randomly selected in the neural network. The three curves in Fig. 12(a) show the medians of the regression results under three different loading conditions.

(2) Uncertainty in the inverse power model: The second step is identifying the coefficients of the inverse power model using the lifespan data. The mapping results are highly sensitive to small variations in the regression coefficients due to the logarithmic transformation in the inverse power model. Although both parameters can influence the results, only the effect of the y-intercept $\log(\alpha)$ is considered in this work because the slopes at different thresholds are nearly identical, as shown in Fig. 12(b). The average slope of −3.5 is determined (solid line in Fig. 12(b)) using the 630 samples of slopes that are calculated using 21 thresholds between 20 and 50 mm and 30 sets of regression models. Once the slope is fixed, the uncertainty in is estimated using the Bayesian approach from 30 samples.

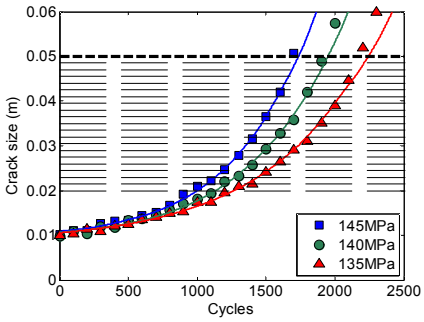

(a) ALT data

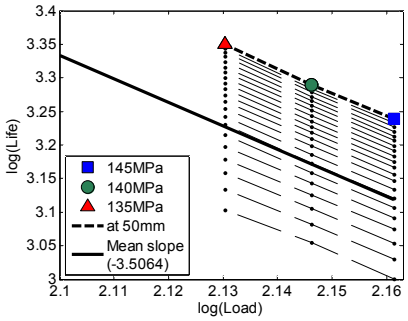

(b) Inverse power model

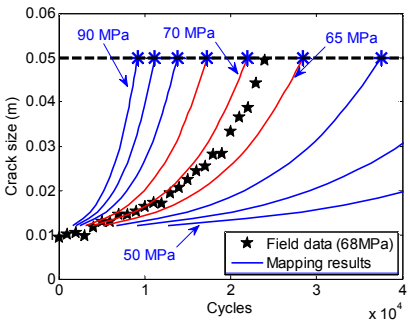

(c) Mapping with estimated life

Fig. 12. Mapping process based on linear relationship between logarithm of life and load.

(3) Uncertainty in the inverse regression process: In the third step, the mapping data in Fig. 12(c) are obtained as lifespan at a given damage threshold, which is the inverse relationship to the data in Fig. 12(a). Therefore, to calculate the damage size for a given cycle, an inverse regression process is required with the mapping data in Fig. 12(c). In the same manner as in the first regression model, the inverse regression process 30 sets of inverse regression models are constructed to consider uncertainty in damage size at given cycles.

Fig. 13(a) shows the uncertainty in the mapping process using confidence intervals. The confidence intervals are calculated from 27000 data ($30 \times 30 \times 30$). In the figure, the 90 %

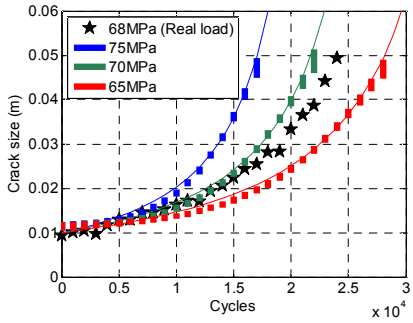

(a) Mapping uncertainty

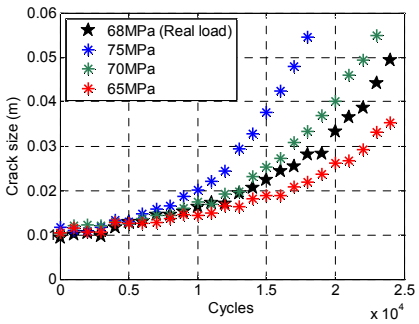

(b) Mapping into field operating conditions

Fig. 13. Mapping between nominal and accelerated condition data.

confidence intervals are shown as the height of the markers. The figure also shows the true damage growths at three different load levels using solid curves. The trend of the transformed data is close to that of the true data, and the magnitude of uncertainty is in a level that is similar to the noise in the field data. Among the 27000 sets of data, any set can be randomly selected for training. The training data are obtained from a well-controlled ALT environment. Hence, all transformed results are close to the true damage trend with a narrow level of uncertainty. The transformed data can be used because they have narrow uncertainty, but they may yield an RUL prediction that is overly narrow relative to the level of noise in the field. To make the transformed data representative of realistic field data, the median trend in the mapping process is obtained, and then the same level of noise in the field data is added to the trend. Fig. 13(b) shows the final data after the addition of noise; these data are used for training in the data-driven approach. The noise is uniformly distributed as $U[-1,1]$ mm . The level of noise is estimated on the basis of the field-measured data of the current system.

Fig. 14 shows the results of damage prediction with mapped data, where the prediction accuracy is similar to the results in case 3 (which uses the given loading information in Fig. 10), but the uncertainties are considerably smaller. The RUL predictions in Fig. 15 show good accuracy (small uncertainty) at every cycle. However, these results are obtained by selecting three loads that are close to the field data up to 10000 cycles. Therefore, RUL results from only 10000 cycles are meaningful. The corresponding metrics of the red curves in Fig. 15 are

Table 6. Prognostics metrics for case 4.

PH ($\alpha = 10\,\%$)	α-λ accuracy ($\alpha = 10\,\%$, $\lambda = 0.5$)	RA ($\lambda = 0.5$)	CRA
14000	**True (0.5000)**	**0.8885**	**0.9050**

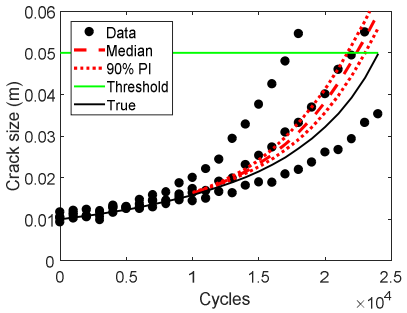

(a) At 10000 cycles

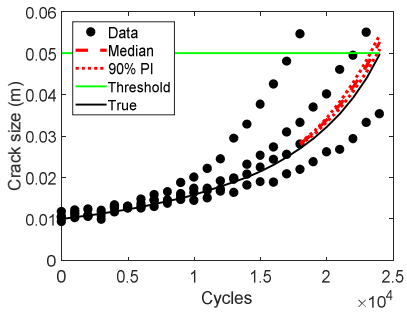

(b) At 18000 cycles

Fig. 14. Damage prediction results of case 4.

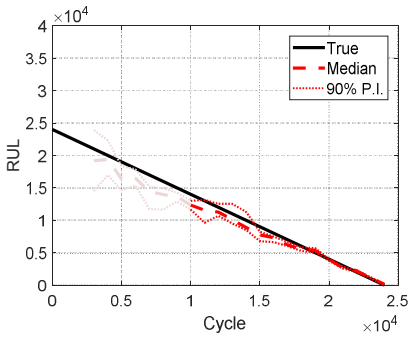

Fig. 15. RUL prediction of case 4.

listed in Table 6.

According to the results of prognostics metrics listed in Tables 2-6, the physics-based approach (case 1) shows the best performance with the same number of data (using ALT data) because case 1 has fewer uncertainty sources (no model and load uncertainties with three [the smallest number] unknown parameters) than other cases, as listed in Table 7. The data-driven approach with mapping data (case 4) has more uncertainty sources (model and load uncertainties with 11 unknown

Table 7. Main sources of uncertainty and prediction performance.

	Case 1	Case 2	Case 3	Case 4
Model	X	X	O	O
Loading	X	O	X	O
Unknown parameter	O (3)	O (4)	O (13)	O (11)
Data for prior/training	ALT	ALT	ALT	Mapping
Metrics	Excellent	Good	Fair	Good

parameters) than other cases. The performance of case 4 is comparable to that of the physics-based approach without loading information (case 2). This finding means that the mapping data that are generated to be close to the field-measured ones for training can compensate for the uncertainties from the model and many unknown parameters. In this context, the prediction results in Figs. 14 and 15 may not be considerably different without mapping data at 75 MPa, which is far from the field one. Also, the prediction accuracy can be increased by updating the training data; that is, training data do not need to be the same as the number of cycles increases. For example, data at 75 MPa can be excluded at 13000 cycles in Fig. 13(b) because the damage level between 75 and the field loading have a large difference. Additional data between 65 and 70 MPa can be generated instead because the mapping data can be readily generated through the mapping process.

Mapping data at field loading can be generated and prediction results improve when the real operating loading is known. These results show that the proposed inverse mapping method can effectively compensate for the inaccuracy caused by insufficient field data. This compensation is achieved by generating a training dataset for nominal loading conditions.

5. Conclusions

In this work, four methods are presented to utilize ALT data for estimating damage degradation model parameters or training mathematical models in data-driven approaches. The new methods are based on available information: (1) the physical model and loading conditions are given; (2) the physical model is given, but loading conditions are uncertain; (3) no physical model is given, but loading conditions are known; and (4) neither physical model nor loading conditions are given. Cases 1 and 3 are considered typical ways of utilizing ALT data in physics-based and data-driven prognostics, respectively. The prediction results are improved by using ALT data in both cases. In case 2, an effective manner of utilizing ALT data is discussed by considering two ways to predict RUL with uncertain loading information. Lastly, a new method is proposed to consider case 4, which is based on a mapping process that uses the inverse power model. The inverse power mapping between field and ALT conditions can compensate for the limited number of in-service damage data, which is the most practical situation.

Acknowledgments

This research was partly supported by the Agency for Defense Development in Korea as a collaborative research agreement under the Integrated Framework of Statistical Simulation and Test.

References

[1] A. K. S. Jardine, D. Lin and D. Banjevic, A review on machinery diagnostics and prognostics implementing condition-based maintenance, *Mechanical Systems and Signal Processing*, 20 (7) (2006) 1483-1510.

[2] D. An, N. H. Kim and J. H. Choi, Practical options for selecting data-driven or physics-based prognostics algorithms with reviews, *Reliability Engineering and System Safety*, 133 (2015) 223-236.

[3] W. Nelson, *Accelerated testing: Statistical models, test plans, and data analysis*, NY: John Wiley & Sons (1990).

[4] J. I. Park and S. J. Bae, Direct prediction methods on lifetime distribution of organic light-emitting diodes from accelerated degradation tests, *IEEE Transactions on Reliability*, 59 (1) (2010) 74-90.

[5] J. R. Celaya, A. Saxena, S. Saha and K. F. Goebel, Prognostics of power MOSFETs under thermal stress accelerated aging using data-driven and model-based methodologies, *Annual Conference of the Prognostics and Health Management Society*, September 25-29, Montreal, Quebec, Canada (2011).

[6] Z. Wang, G. Zhai, X. Huang and X. Ye, Study on feasibility of storage accelerated testing based on parameter degradation for aerospace relays, *IEEE International Conference on Prognostics and System Health Management (PHM)*, May 23-25, Beijing, China (2012).

[7] H. Skima, K. Medjaher and N. Zerhouni, Accelerated life tests for prognostic and health management of MEMS devices, *2nd European Conference of the Prognostics and Health Management Society*, July 8-10, Nantes, France (2014).

[8] J. Luo, K. R. Pattipati, L. Qiao and S. Chigusa, Model-based prognostic techniques applied to a suspension system, *IEEE Transactions on System, Man and Cybernetics*, 38 (5) (2008) 1156-1168.

[9] M. A. Schwabacher, A survey of data-driven prognostics, *AIAA Infotech@Aerospace Conference*, September 26-29, Arlington, VA (2005).

[10] J. Yan and J. Lee, A hybrid method for on-line performance assessment and life prediction in drilling operations, *IEEE International Conference on Automation and Logistics*, August 18-21, Jinan, Shandong , China (2007).

[11] T. Bayes, An essay towards solving a problem in the doctrine of chances, *Philosophical Transactions*, 53 (1763) 370-418.

[12] R. E. Kalman, A new approach to linear filtering and prediction problems, *Transaction of the ASME-Journal of Basic Engineering*, 82 (1960) 35-45.

[13] S. J. Julier and J. K. Uhlmann, Unscented filtering and nonlinear estimation, *Proceedings of the IEEE*, 92 (3) (2004) 401-422.
[14] A. Doucet, N. D. Freitas and N. J. Gordon, *Sequential Monte Carlo methods in practice*, NY: Springer-Verlag (2001).
[15] S. C. Kramer and H. W. Sorenson, Bayesian parameter estimation, *IEEE Transactions on Automatic Control*, 33 (2) (1988) 217-222.
[16] D. An, J. H. Choi and N. H. Kim, Prognostics 101: A tutorial for particle filter-based prognostics algorithm using Matlab, *Reliability Engineering and System Safety*, 115 (2013) 161-169.
[17] J. A. DeCastro, L. Tang, K. A. Loparo, K. Goebel and G. Vachtsevanos, Exact nonlinear filtering and prediction in process model-based prognostics, *Annual Conference of the Prognostics and Health Management Society*, September 27 - October 1, San Diego, CA (2009).
[18] E. Zio and F. D. Maio, A data-driven fuzzy approach for predicting the remaining useful life in dynamic failure scenarios of a nuclear system, *Reliability Engineering and System Safety*, 95 (2010) 49-57.
[19] K. Chakraborty, K. Mehrotra, C. K. Mohan and S. Ranka, Forecasting the behavior of multivariate time series using neural networks, *Neural Networks*, 5 (1992) 961-970.
[20] X. Yao, Evolving artificial neural networks, *Proceedings of the IEEE*, 87 (9) (1999) 1423-1447.
[21] D. C. M. Dickson and H. R. Waters, Gamma processes and finite time survival probabilities, *Astin Bulletin*, 23 (2) (1993) 259-272.
[22] L. R. Rabiner, A tutorial on hidden Markov models and selected applications in speech recognition, *Proceedings of the IEEE*, 77 (2) (1989) 257-286.
[23] M. Seeger, Gaussian processes for machine learning, *International Journal of Neural Systems*, 14 (2) (2004) 69-106.
[24] S. Mohanty, R. Teale, A. Chattopadhyay, P. Peralta and C. Willhauck, Mixed Gaussian process and state-space approach for fatigue crack growth prediction, *International Workshop on Structural Heath Monitoring*, 2 (2007) 1108-1115.
[25] M. E. Tipping, Sparse Bayesian learning and the relevance vector machine, *Journal of Machine Learning Research*, 1 (2001) 211-244.
[26] V. T. Tran and B. S. Yang, Data-driven approach to machine condition prognosis using least square regression tree, *Journal of Mechanical Science and Technology*, 23 (2009) 1468-1475.
[27] D. Svozil, V. Kvasnička and J. Pospíchal, Introduction to multi-layer feed-forward neural networks, *Chemometrics and Intelligent Laboratory Systems*, 39 (1997) 43-62.
[28] P. C. Paris and F. Erdogan, A critical analysis of crack propagation laws, *ASME Journal of Basic Engineering*, 85 (1963) 528-534.
[29] J. C. Newman Jr., E. P. Phillips and M. H. Swain, Fatigue-life prediction methodology using small-crack theory, *International Journal of Fatigue*, 21 (1999) 109-119.
[30] D. An, J. H. Choi and N. H. Kim, Identification of correlated damage parameters under noise and bias using Bayesian inference, *Structural Health Monitoring*, 11 (3) (2012) 293-303.
[31] A. Saxena, J. Celaya, B. Saha, S. Saha and K. Goebel, On applying the prognostic performance metrics, *Annual Conference of the Prognostics and Health Management Society*, September 27 - October 1, San Diego, CA (2009).

Dawn An received her B.S. and M.S. in mechanical engineering from the Korea Aerospace University in 2008 and 2010, respectively. She started a joint Ph.D. at Korea Aerospace University and the University of Florida in 2011 and received a jointly conferred Ph.D. in 2015. She then became Postdoctoral Associate at the University of Florida for 1 year. She is now Senior Researcher at the Korea Institute of Industrial Technology. Her current research focuses on prognostics and health management for not only machines but also the human body.

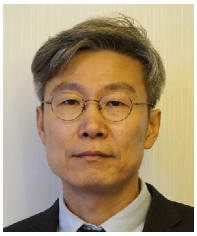

Joo-Ho Choi received his B.S. in mechanical engineering from Hanyang University in 1981 and his M.S. and Ph.D. in mechanical engineering from the Korea Advanced Institute of Science and Technology in 1983 and 1987, respectively. In 1988, he was Postdoctoral Fellow at the University of Iowa. He joined the School of Aerospace and Mechanical Engineering at Korea Aerospace University, Korea, in 1997 and is now Professor. His current research focuses on reliability analysis, design for lifetime reliability, and prognostics and health management.

Nam Ho Kim received his B.S. in mechanical engineering from Seoul National University in 1989, his M.S. in mechanical engineering from the Korea Advanced Institute of Science and Technology in 1991, and his Ph.D. in mechanical engineering from the University of Iowa in 1999. He was Postdoctoral Associate at the University of Iowa from 1999 to 2001. He joined the Department of Mechanical & Aerospace Engineering at the University of Florida in 2002 and is now Associate Professor. His current research focuses on design under uncertainty, design optimization of automotive NVH problem, shape DSA of transient dynamics (implicit/explicit), and structural health monitoring.